

pubs.acs.org/JPCC Perspective

Probing Carrier Transport in Layered Perovskites with Nonlinear Optical and Photocurrent Spectroscopies

Ninghao Zhou, [†] Zhenyu Ouyang, [†] Meredith McNamee, Olivia F. Williams, Zhenkun Guo, Liang Yan, Jun Hu, Wei You, and Andrew M. Moran*



Cite This: J. Phys. Chem. C 2021, 125, 8021–8030



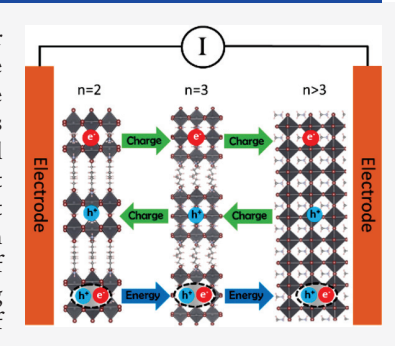
ACCESS

III Metrics & More

Article Recommendations

Supporting Information

ABSTRACT: Interest in layered perovskite quantum wells is motivated by their potential for use in optoelectronic devices. In these systems, the smallest and largest quantum wells are most concentrated near opposing electrodes in photovoltaic cells. Coincident gradients in the energy levels and quantum well concentrations promote the funneling of electronic excitations and charge carriers through space. In this Perspective, we describe the development of several nonlinear optical techniques designed to elucidate the relaxation processes induced by light absorption in layered perovskite systems. Transient absorption microscopy provides insight into carrier diffusion and two-body recombination processes, whereas two-dimensional action spectroscopies are used to correlate elementary relaxation mechanisms to practical metrics of photovoltaic device performance. Our experiments suggest that charge carrier funneling processes do not facilitate long-range transport due to trapping. Rather, the bulklike phases of the films absorb light and transport carriers without participation of the smallest quantum wells.



■ INTRODUCTION

Bulk organohalide perovskites have demonstrated great potential for use in optoelectronic devices such as solar cells and light-emitting diodes. 1-6 These materials offer favorable light absorption coefficients and tunable band gaps; however, long-term stability and toxicity remain significant challenges. One class of systems presently under development involves mixtures of two-dimensional perovskite quantum wells termed "layered perovskites." These two-dimensional systems possess large exciton binding energies and are more resistant to moisture than the corresponding bulk materials. 12,13 In addition, interactions between quantum wells give rise to a multitude of photoinduced relaxation processes including electron transfer, energy transfer, defect-assisted recombination, and spontaneous emission. 14-21 Disentangling these mechanisms with conventional transient absorption spectroscopy has proven quite challenging due to ambiguities in signal interpretation. 14,15,17-20,22 Moreover, the electronic states and processes important for the function of a photovoltaic cell do not necessarily yield spectroscopic signatures with significant intensities. The complexity of layered perovskite materials has motivated applications of "action spectroscopies" capable of directly targeting the functionally relevant processes induced by light absorption. ^{23–26} In these experiments, nonlinearities in spontaneous processes of interest (e.g., photocurrent, fluorescence emission) are directly detected to reveal the microscopic behaviors that underlie the performances of photovoltaic devices.²⁷⁻³⁴

In this Perspective, we describe the elucidation of lightinduced energy and charge transport mechanisms in layered perovskites using a variety of nonlinear spectroscopies. First, we present a transient absorption microscopy method designed to reveal carrier diffusion, two-body recombination, and exciton dissociation processes in layered perovskite films. 35,36 Our measurements show that motions of the charge carriers are sensitive to the thicknesses of the quantum wells in addition to extrinsic factors such as grain boundaries and structural disorder. Second, we have developed nonlinear action spectroscopies to decompose the optical responses of photovoltaic cells into productive (photocurrent) and lossy (fluorescence) processes. ^{23–25} Applications of these techniques are motivated by the inability of transient absorption experiments to distinguish energy and charge transfer mechanisms. Most recently, we have shown that trajectoryspecific carrier mobilities can be determined for layered perovskite systems by cycling the laser pulse sequences and external biases applied to a photovoltaic cell.²⁶ These experiments suggest promise in a new family of techniques that combine multidimensional spectroscopies with device measurements.

Received: January 24, 2021 Revised: March 4, 2021 Published: April 2, 2021





Coincidence between the concentrations and electronic structures of layered perovskite quantum wells gives rise to energy and charge funneling behaviors. For example, the leadiodide perovskite quantum wells targeted in our work are described by the general chemical formula $A_nMA_{n-1}Pb_nI_{3n+1}$, where A is an organic cation and MA is methylammonium (CH₃NH₃⁺). With insulating organic cations such a butyl ammonium or phenyl ethylammonium, quantum wells in which n = 2, 3, and 4 exhibit exciton resonances near 570, 600, and 640 nm, respectively. Exciton binding energies also decrease as the value of n increases due to a combination of dimensionality and the dielectric environment. 37,38 For example, quantum wells with n = 2, 3, and 4 have exciton binding energies of approximately 251, 177, and 157 meV, respectively.³⁸ Because of these differences, the behaviors of layered perovskite systems are quite sensitive to the concentration distributions of quantum wells with different sizes. In solution-processed films, the smallest and largest quantum wells are primarily concentrated near the glass and air interfaces, respectively (i.e., near opposing electrodes in a photovoltaic device). 14,17,18,36 As indicated in Figure 1, the

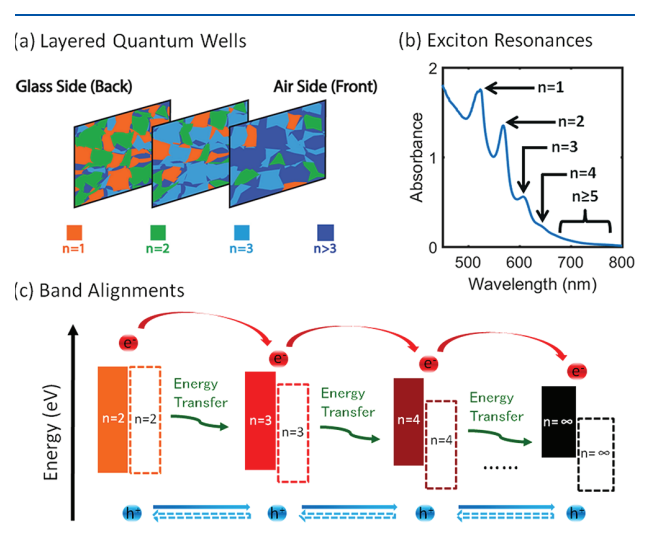


Figure 1. Concentration distributions and electronic structures of layered perovskite systems. (a) Larger and smaller quantum wells are concentrated near opposite faces of the films. (b) The thicknesses and exciton resonance wavelengths of quantum wells increase with the index, n. (c) Staggering of the band gaps and energy levels promotes energy and electron funneling through space and toward the largest quantum wells. The direction of hole transport is still under investigation because a consensus has not been reached regarding whether the system possesses Type I (shaded rectangles) or Type II (open rectangles) band alignments.

average band gaps and conduction band levels decrease from the glass to air sides of a film, thereby promoting energy and electron transport in the same direction. A consensus has not been reached regarding the preferential direction of hole transport. Holes are predicted to transfer from the smallest to largest quantum wells with Type I band alignments (i.e., from the glass to air interfaces), whereas the opposite is true for a Type II configuration. Recent theoretical work suggests that disordered systems may exhibit a mixture of Type I and II band alignments. ³⁹

CARRIER DIFFUSION AND RECOMBINATION REVEALED BY TRANSIENT ABSORPTION MICROSCOPY

Knowledge of carrier diffusion in layered perovskites is motivated by implications for electron and hole mobilities when subjected to an electric field.⁴⁰ Transient absorption microscopy has been demonstrated as a powerful new approach for studying carrier diffusion in nanoparticles and films. 41-52 In these experiments, the pump beam is usually focused with a microscope objective and a probe beam is raster scanned to image carrier dynamics. Such point-by-point data acquisition is readily accomplished using laser systems with MHz repetition rates. We have developed an alternate widefield microscopy approach that is compatible with an available 1 kHz, titanium sapphire laser. This laser system is coupled to an automated spectral filter, which supplies color-tunable laser pulses in the visible spectral range for multiple experimental techniques (e.g., conventional transient absorption and action spectroscopies). The wavelengths of the laser pulses may be tuned into the resonances of specific quantum wells to compare their diffusivities and recombination mechanisms.

Our approach to transient absorption microscopy employs two multiplexing methods to minimize data acquisition times.³⁵ As shown in Figure 2a, a diffractive optic splits a

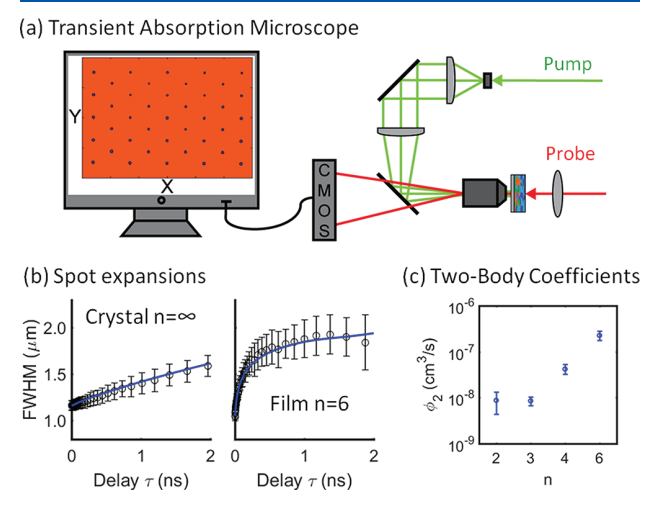


Figure 2. Carrier dynamics are probed with a diffractive optic-based transient absorption microscope. (a) Layered perovskite films are photoexcited at 41 spots, which are probed with a counterpropagating beam. Wide-field signal detection is enabled by a two-dimensional CMOS array detector. (b) Carrier diffusion and two-body recombination dominate in crystals and films, respectively. (c) Two-body recombination coefficients increase with the index of the quantum well, n. This behavior is attributed to the greater probability of exciton dissociation and free carrier recombination in larger quantum wells. Reprinted with permission from refs 35 and 36. Copyrights 2018 and 2019 American Chemical Society.

color-tunable pump beam into 41 beams, which are focused to 1 $\mu \rm m$ spot sizes on the sample surface. Conducting 41 experiments in parallel is advantageous for studies of heterogeneous films because statistics may be quickly compiled. In addition, counter-propagation of the pump and probe beams through the sample enables wide-field signal detection with a two-dimensional CMOS array detector on a shot-to-shot basis. Notably, the probe beam is focused to a spot size much larger than the field-of-view to avoid undesired

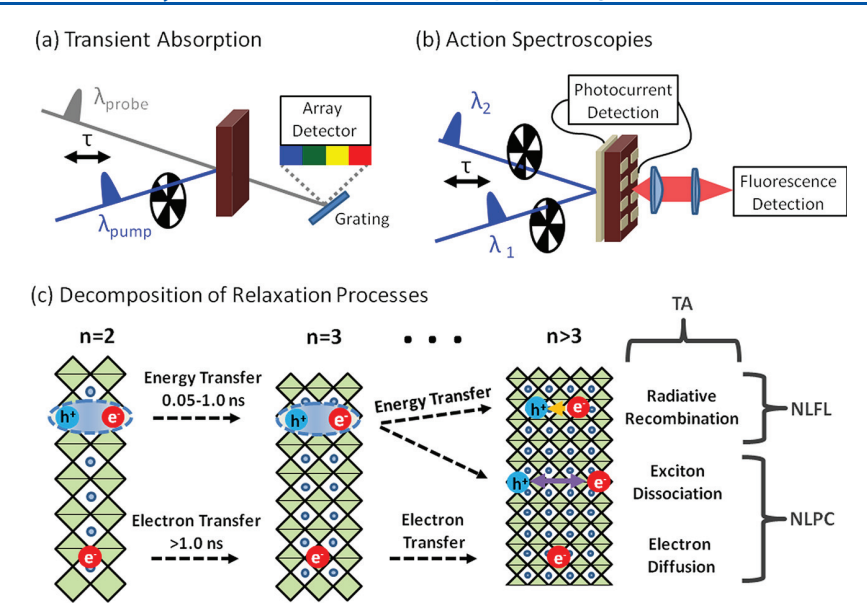


Figure 3. Action spectroscopies correlate ultrafast relaxation mechanisms to the fates of the electronic excitations. (a) Conventional transient absorption (TA) setup with dispersed detection is shown. (b) A pair of color-tunable laser pulses induces nonlinear photocurrent (NLPC) and fluorescence (NLFL) signals. (c) TA experiments are sensitive to all photoexcited populations at delay time, τ . The contribution of a particular species depends on its concentration and extinction coefficient rather than its functional significance. NLFL and NLPC experiments are primarily sensitive to energy and charge transport, respectively. In effect, the optical response detected by TA spectroscopy is decomposed into lossy and productive components by NLFL and NLPC measurements, respectively. Panel (c) is adapted with permission from ref 25. Copyright 2020 American Institute of Physics.

intensity-dependent effects. The pump and probe beams originate in a continuum generated by filamentation in argon gas. Automated spectral filtering devices are used to select 5 nm wide portions of the pump and probe beams for use in experiments.³⁵

Behaviors of electronic excitations in layered perovskite films were compared to those in a variety of single crystals to understand the influence of grain boundaries and disorder on carrier motions. 35,36 In crystals, we found that carrier diffusion gives rise to a quasi-linear growth in the photoexcited spot widths on the nanosecond time scale (see Figure 2b). These dynamics correspond to diffusivities in good agreement with earlier literature. 41,42,53 In contrast, measurements conducted on films show that two-body recombination induces a nonlinear rise in the spot widths on the subnanosecond time scale. Control experiments confirm that these dynamics are unrelated to ballistic transport in the present systems.³⁶ Rather, in films, the spot widths expand because the two-body recombination rate increases with the carrier density, which is greatest in the centers of the photoexcited regions. Decay mechanisms that scale as the square of carrier density include radiative relaxation and trap-assisted Auger recombination. We attribute two-body recombination in the films to the trapping of carriers within individual disordered grains based on the absence of such behavior in the crystals. The standard deviations shown in Figure 2b correspond to 205 measurements. Fast acquisition of statistical information is an advantage of this diffractive optic-based approach.

Interestingly, our transient absorption microscopy experiments show that quantum wells with different sizes possess markedly different two-body recombination coefficients in films.³⁶ As indicated in Figure 2c, our measurements establish that the prevalence of two-body recombination increases with the index of the quantum well, *n*. Minimal two-body

recombination is observed in quantum wells with n=2 and 3; however, the recombination coefficients are more than an order of magnitude larger in quantum wells with n=6. We attribute this behavior to the smaller exciton binding energies found in larger quantum wells. For example, the fractions of dissociated excitons predicted by the Saha equation are approximately 2% and 50% in systems with n=2 and ∞ , respectively. Thus, our data suggest that the subnanosecond, nonlinear rises in the spot widths observed in larger quantum wells represent two-body recombination of free charge carriers. Interactions between excitons in the smaller quantum wells (n<4) do not produce such significant density-dependent effects.

■ DISTINGUISHING PRODUCTIVE AND LOSSY RELAXATION PROCESSES BY NONLINEAR ACTION SPECTROSCOPIES

Photoexcitation induces a multitude of relaxation processes in layered perovskites, which have proven difficult to disentangle by transient absorption spectroscopy (e.g., energy transfer, charge transfer, spontaneous emission, many-body recombination). 5,14,15,17-21,24 Although dominant carrier funneling dynamics were suggested in early work, it is now clear that energy transfer processes have significant yields for the smallest quantum wells due to their higher binding energies and transition dipole couplings.³⁸ Transient absorption cross-peaks were previously suggested to represent extraordinary hole transfer processes; however, we have shown these resonances to be natural consequences of transition dipole couplings²⁴ similar to those observed in molecular aggregates and photosynthetic complexes. 55,56 Moreover, global fits of data based on explicit response functions suggest that 40-50% of the electronic excitations in smaller quantum wells participate in energy transfer processes. ^{17,18} The remainder of the excitations relax through a combination of defect-assisted

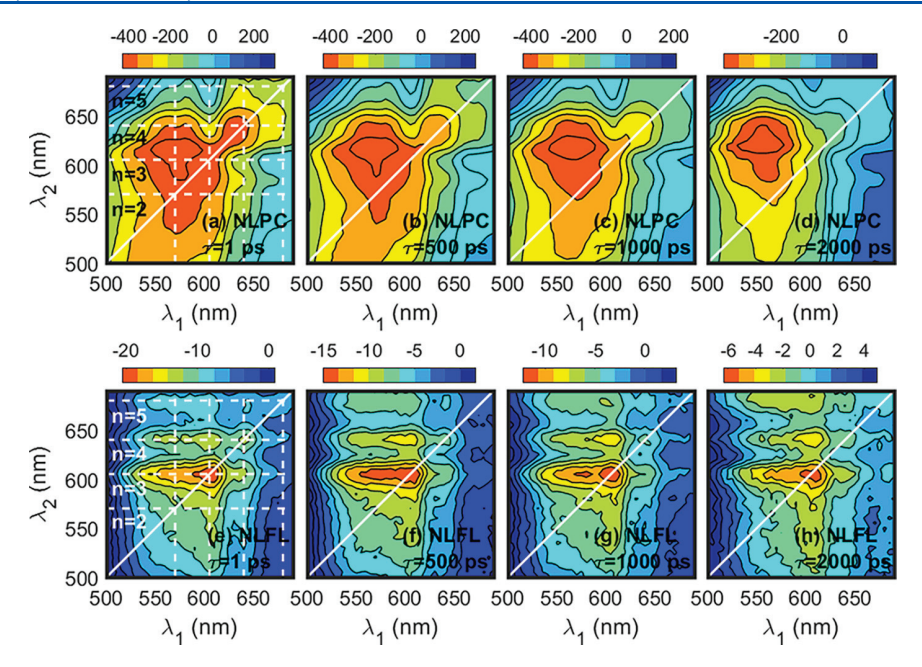


Figure 4. Two-dimensional NLPC (top) and NLFL (bottom) spectra are acquired at (a), (e) 1 ps; (b), (f) 500 ps; (c), (g) 1000 ps; (d), (h) 2000 ps. Electron and energy transfer processes induce red shifts along the λ_2 axis for the NLPC and NLFL spectra, respectively. For both axes, peaks associated with the n = 2, 3, 4, and 5 quantum wells are located at 570, 600, 640, and 680 nm. The NLPC and NLFL signals are reported in units of nA and mV, respectively. Reprinted with permission from ref 24. Copyright 2020 American Chemical Society.

recombination, spontaneous emission, and charge carrier funneling dynamics.

Contributions from energy transfer processes are consistent with the basic physics of the systems. Layered perovskites consist of quantum wells with large transition dipoles (≥ 10 D)⁵⁷ in close proximities (~ 1 nm). The Coulombic couplings are on the order of 10s of millielectronvolts under the assumption of an inverse cubic dependence on the donor—acceptor separation; ^{17,24} however, Scholes and co-workers have shown that the coupling scales as the inverse square of the distance between the donor and acceptor for cofacial geometries. Because the couplings that drive charge transfer decrease exponentially with distance, it should be anticipated that energy transfer outcompetes charge transfer on short time scales. S8,59

Temperature variation can be a powerful approach for distinguishing parallel relaxation mechanisms in layered perovskites.²² Marcus' equation for charge transfer possesses well-known activated and activationless regimes. 58,59 In addition, it has been established that Förster's rate formula exhibits a temperature dependence originating in the spectral overlap between the donor and acceptor. $^{60-62}$ These earlier works suggest that the temperature dependence of energy transfer will be most pronounced in systems like layered perovskites, where the nondegenerate donor and acceptor spectra have narrow line widths. Fluctuations in energy gaps, which promote transitions by temporarily bringing the energy donor and acceptor resonances into degeneracy, scale as the square root of temperature under the assumption of Gaussian statistics. 63,64 Whereas the homogeneous component of the line width is sensitive to temperature, static disordered environments can give rise to temperature-independent inhomogeneous line widths (i.e., the subensembles cannot be exchanged by spectral diffusion). In the Supporting Information, we present calculations that illustrate how temperature can influence energy transfer processes in layered perovskites.

Notably, the temperature dependence of energy transfer mechanisms does not rule out parallel charge transfer or Dexter energy transfer processes.

Transient absorption signals are primarily sensitive to energy transfer processes because excitons dominate the nonlinear optical responses. For this reason, we have developed nonlinear fluorescence (NLFL) and photocurrent (NLPC) spectroscopies to separately target energy and charge transfer mechanisms. The information content associated with these techniques is illustrated in Figure 3. In a transient absorption experiment, the populations of reactants, intermediates, and products are tracked by varying the experimentally controlled delay time, τ . The signal intensity associated with a particular species depends only on its concentration and extinction coefficient for light absorption. In our action spectroscopies, two laser pulses with a variable delay time are similarly applied to a photovoltaic cell; however, both beams must be chopped to isolate the nonlinear response because the transmission of the second laser pulse is not detected. Rather, the signal (either photocurrent or fluorescence intensity) is cycled between four conditions: pulse 1 only (S_1) , pulse 2 only (S_2) , pulses 1 and 2 (S_{1+2}) , and both pulses blocked (S_0) . The nonlinear response is isolated by evaluating the linear combination, $S_{Action} = S_{1+2}$ – $S_1 - S_2 + S_0$. In effect, this pair of action spectroscopies decomposes the optical response into productive (photocurrent) and lossy (fluorescence) relaxation processes.

Our recent applications of NLPC and NLFL spectroscopies to layered perovskite systems demonstrate the utilities of the methods.^{23–26} The spectra presented in Figure 4 exemplify the complementary information provided by these two detection channels. The NLPC spectra exhibit broader line widths and smaller contributions from excitons when compared to the corresponding NLFL spectra. In fact, the suppression of exciton resonances is not unique to nonlinear action spectroscopies. Linear transmission and external quantum efficiency (EQE) spectra acquired for layered perovskites

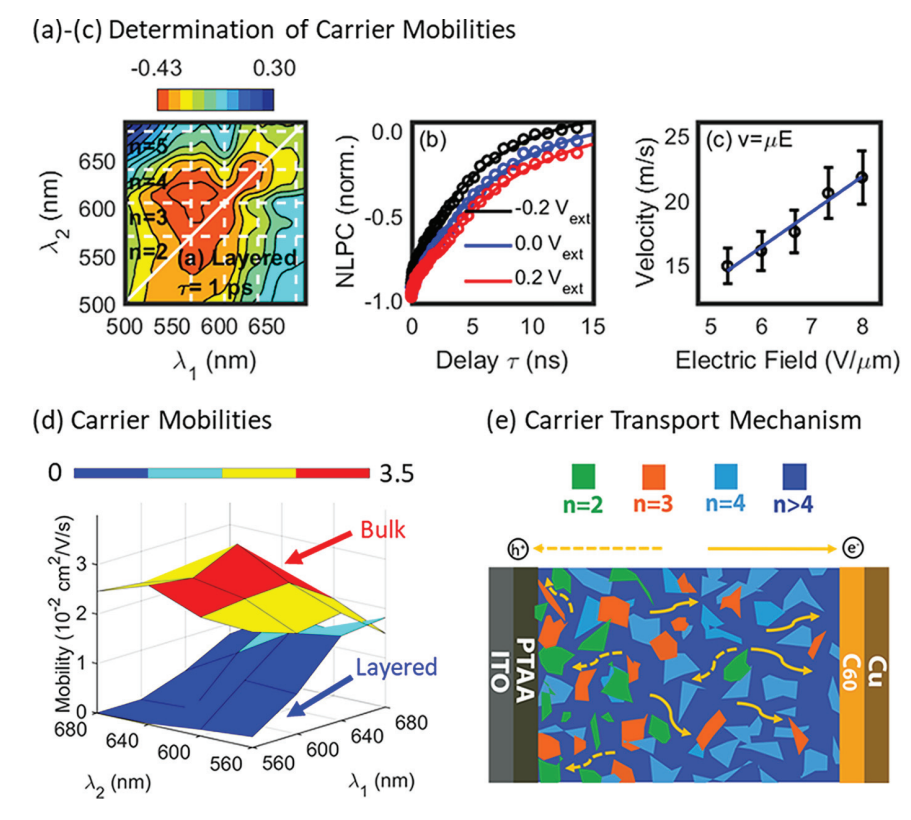


Figure 5. NLPC spectroscopy is used to determine 2D carrier mobility surfaces for layered and bulk perovskites. (a)—(c) The external bias applied to the cell is varied to extract drift velocities. Linear fits of the velocities versus electric fields yield the carrier mobilities. (d) Quantum well-specific carrier mobilities determined for layered perovskites reveal a pronounced asymmetry above and below the diagonal of the 2D mobility spectrum. The mobilities are smallest when the charge transport processes are initiated by photoexcitation of smaller quantum wells (n = 2-3). The mobility surface determined for a bulk perovskite is relatively flat and does not approach zero in any region of the spectrum. (e) NLPC measurements suggest that electron and hole transport occur in the phases of the thickest quantum wells in layered perovskite-based photovoltaic cells. Charge carrier funneling processes do not contribute to the photocurrent. Reprinted with permission from ref 26. Copyright 2021 American Chemical Society.

possess similar differences in line widths, wherein the contributions of excitons to the EQE are diminished compared to the linear transmission spectra. We hypothesize that the discrepancy between transmission and EQE spectra originates in the large exciton binding energies, which are close to 10 times $k_{\rm B}T$ in the smaller quantum wells. That is, the large exciton binding energies increase the probability that light absorption will result in spontaneous emission rather than exciton dissociation. This interpretation is consistent with the intense steady-state fluorescence emission observed for the smallest quantum wells in layered perovskite films. 17,18

The NLPC spectra possess peaks near the exciton resonance wavelengths of 570, 600, and 640 nm. For example, at $\tau=1$ ps, the peak associated with the n=4 quantum wells near $\lambda_1=\lambda_2=640$ nm appears well-resolved because the continuum transitions associated with smaller quantum wells are found at shorter wavelengths. As the delay time increases, the signal intensity red shifts along the λ_2 axis at $\lambda_1=570$ nm. This region of the spectrum is primarily associated with excitations initially located in n=2 system ($\lambda_1=570$ nm); however, the line widths are broad, so the dynamics cannot be unambiguously assigned to specific quantum wells (e.g., n=2 to n=3 electron transfer). Nonetheless, the nanosecond time scale of the red shift observed by NLPC spectroscopy is consistent with the direction of electron transfer processes depicted in Figure 1.

The NLFL spectra presented in the bottom row of Figure 4 reveal enhanced contributions from exciton resonances, which have much narrower line widths than those found in the NLPC spectra. For the slice of the NLFL spectra at $\lambda_1 = 600$ nm (n =3), the progression of peaks observed at $\lambda_2 = 600$, 640, and 680 nm corresponds to the n = 3, 4, and 5 quantum wells, respectively. Each of these quantum wells is populated at $\tau = 1$ ps; however, this primarily occurs by way of direct photoexcitation of higher-energy continuum states as opposed to nonradiative transitions between quantum wells. 17,18 The initial condition, wherein each of the quantum wells is significantly populated by the first laser pulse, partly obscures observations of energy transfer-induced red shifts in the signal intensity. At $\tau = 500$ ps, signal intensity has accumulated in a cross peak at $\lambda_1 = 600$ nm and $\lambda_2 = 640$ nm due to energy transfer processes. In contrast, the cross peak at $\lambda_1 = 600$ nm and $\lambda_2 = 680$ nm grows more slowly because the n = 5quantum well is populated through a sequence of energy transfer steps (i.e., n = 3 to n = 4 transitions occur before n = 4to n = 5). These interpretations of the NLFL spectra have been confirmed by combining a response function-based model with the relaxation scheme summarized in Figure 3.²⁵

Although NLPC spectroscopy reveals signatures of carrier funneling, it is not clear on the basis of the measurements in Figure 4 that these processes enhance the performance of a photovoltaic cell. That is, carriers photoexcited in the layered

perovskite system may reach the electrodes by a variety of trajectories that do not involve funneling. In addition, the temporal profiles of NLPC signals are influenced by processes including carrier drift, diffusion, spontaneous emission, and two-body recombination. Because the drift velocity scales linearly with the applied electric field, the pulse sequence and external bias applied to the device may be cycled to decompose mobility of the material into contributions from specific pathways. Like a conventional time-of-flight method, 65 carrier transport is initiated by photoexcitation of the active layer in NLPC spectroscopy; however, information regarding the trajectory is gathered by applying a second, intervening laser pulse before the carriers are injected into the transport layers. Layered perovskites are ideally suited for this approach because trajectories can be distinguished by tuning the laser pulses into separate components of the active layer.

The procedure used to determine carrier mobilities is illustrated in Figure 5. The wavelengths of the two pulses are tuned into the exciton resonances designated by the 16 points of intersection in Figure 5a. The signal magnitude decreases as the delay time increases because photoexcited carriers are cleared from the active layer; however, this may occur by photocurrent generation in addition to a variety of excitedstate deactivation processes. With inspiration from conventional time-of-flight methods, 66,67 the external bias applied to the photovoltaic cell is cycled from -0.2 to +0.2 V to target carrier drift. The velocities are determined for each of the external biases by dividing the active layer thickness by the average decay times, which are determined by fitting the decay profiles to biexponential functions. The mobilities are then obtained by fitting the velocity versus the electric field to a straight line. Here, the electric field is set equal to the ratio of the potential and active layer thickness, where the overall potential is given by the sum of the internal and external biases. Because the internal bias has a negative sign (-1.0 V), the shortest decay times are measured with an external bias of -0.2V in Figure 5b.

The mobilities determined for the layered perovskite system exhibit a significant asymmetry above and below the diagonal of the 2D NLPC spectrum. Signals acquired above the diagonal represent processes in which electrons transfer from smallest to largest quantum wells as depicted in Figure 1. For example, the mobility of zero measured at the cross peak between the n = 2 and 5 quantum wells ($\lambda_1 = 570$ nm and $\lambda_2 =$ 680 nm) reflects insensitivity of the electron funneling process to the external bias.²⁶ The temporal profiles of NLPC signals measured in this region of the spectrum do not decay monotonically because of carrier trapping in the domains occupied by the smallest quantum wells.²⁶ In contrast, carrier transport is initiated in the largest quantum wells when the first laser pulse is tuned to longer wavelengths. We do not assign the large mobilities measured below the diagonal of the 2D NLPC spectrum to an extraordinary hole transfer mechanism (see Figure 1). Rather, we suggest that the thickest quantum wells absorb light and transport the carriers to the chargeselective layers without transitions into other phases of the material. The larger quantum wells contribute off-diagonal responses because the resonances with continuum states span the full visible spectral range. For example, the quantum well with n = 5 exhibits an intense response with $\lambda_1 = 680$ nm (exciton) and $\lambda_2 = 570$ nm (continuum states).

Mobilities measured for layered and bulk perovskite systems are compared in Figure 5d. Unlike the layered perovskite, the

2D mobility surface measured for the bulk perovskite is relatively flat and does not possess regions of zero mobility. Insensitivity of the mobilities to the excitation wavelengths is expected for the bulk perovskite because carrier cooling is fast compared to the transit time through the active layer. These results are also in good agreement with the electron mobility of a bulk perovskite obtained by measuring the steady-state space charge-limited current (0.012 cm²/V/s);⁶⁸ however, photoluminescence quenching experiments, which are not conducted with photovoltaic devices, yield mobilities that are 50–100 times larger than those determined by NLPC spectroscopy. We attribute this discrepancy between *in situ* and *ex situ* measurements to contributions from the electrodes, interfaces with the transport layers, and space-charge effects in photovoltaic devices.

Our results suggest the transport mechanism depicted in Figure 5e dominates photocurrent generation in layered perovskite systems. Carrier funneling processes do not facilitate long-range transport because of trapping in the domains occupied by the smallest quantum wells. Rather, photocurrent generation is most efficient when the largest quantum wells absorb light and transport the carriers without transitions into phases associated with smaller quantum wells. In addition, we find that photoexcitation of the smallest quantum wells is a major source of energy loss in photovoltaic devices. As evidenced by steady-state fluorescence spectra, the smallest quantum wells are likely to relax by spontaneous emission because they have the largest exciton binding energies and transition dipoles. Moreover, the concentration profiles of the smallest quantum wells do not span the full thicknesses of the active layers, leading to "dead ends" in the carrier trajectories.36

CONCLUSIONS

Overall, the experiments summarized in this perspective article support the following physical insights into relaxation processes induced by light absorption in layered perovskite films and photovoltaic devices:

- (i) Dynamics in the spatial distributions of photoexcited charge carriers are primarily influenced by two-body recombination in films because of disorder and grain boundaries. Carrier diffusivity is 10–100 times greater in single crystals compared to solution-processed films.
- (ii) Energy funneling is a subnanosecond process, whereas charge carrier funneling occurs at later times.
- (iii) Charge carrier funneling does not contribute to longrange transport because of trapping in the domains occupied by the smallest quantum wells.
- (iv) Photocurrent generation in layered perovskite-based devices is dominated by processes in which the largest quantum wells absorb light and transport carriers without transitions into phases associated with smaller quantum wells.
- (v) The smallest quantum wells function as debris in photovoltaic devices. These systems are likely to relax by spontaneous emission and do not have concentration profiles spanning the full active layer of a device.

In conclusion, our investigations of layered perovskites suggest that the concentration profiles of the individual quantum wells are not tailored to produce functionally relevant charge carrier funnels. Alternate approaches must be considered to exploit the optoelectronic properties of these

systems. One aspect of layered 2D perovskites, which sets them apart from their bulk 3D counterparts, is the accommodation of large organic molecules between the layers of inorganic octahedra. Thus far, we have investigated systems in which insulating organic molecules, which are transparent in the visible spectral range, fill the interstitial spaces between quantum wells; however, organic chromophores with smaller band gaps can be substituted to promote out-of-plane transport processes. 70-75 Energy transfer and exciton delocalization can be enhanced in systems where the donor and acceptor sites possess degenerate electronic resonances. In addition, the individual energy levels can be varied to promote charge transfer between the inorganic and organic phases of the materials. Because the couplings that drive charge transfer transitions are short-range in nature, charge carrier mobilities can be significantly enhanced by incorporating organic chromophores. Studies of crystals with well-characterized structures will be necessary to distinguish in-plane and outof-plane charge transport in materials with such hybridized electronic structures. Extending the NLPC method from the nanosecond to microsecond time scale will enable studies of crystals, which will have transit times greater than the systems targeted in Figure 5 due to larger thicknesses.

ASSOCIATED CONTENT

Supporting Information

The Supporting Information is available free of charge at https://pubs.acs.org/doi/10.1021/acs.jpcc.1c00654.

Energy transfer rates are computed as a function of temperature using parameters associated with layered perovskite quantum wells (PDF)

AUTHOR INFORMATION

Corresponding Author

Andrew M. Moran — Department of Chemistry, University of North Carolina at Chapel Hill, Chapel Hill, North Carolina 27599, United States; oorcid.org/0000-0001-7761-7613; Email: ammoran@email.unc.edu

Authors

Ninghao Zhou — Department of Chemistry, University of North Carolina at Chapel Hill, Chapel Hill, North Carolina 27599, United States; orcid.org/0000-0002-7255-282X

Zhenyu Ouyang — Department of Chemistry, University of North Carolina at Chapel Hill, Chapel Hill, North Carolina 27599, United States; orcid.org/0000-0001-9549-0353

Meredith McNamee — Department of Chemistry, University of North Carolina at Chapel Hill, Chapel Hill, North Carolina 27599, United States; orcid.org/0000-0003-4432-5870

Olivia F. Williams – Department of Chemistry, University of North Carolina at Chapel Hill, Chapel Hill, North Carolina 27599, United States; oorcid.org/0000-0001-5364-7703

Zhenkun Guo — Department of Chemistry, University of North Carolina at Chapel Hill, Chapel Hill, North Carolina 27599, United States; Occid.org/0000-0003-1905-5557

Liang Yan — Department of Chemistry, University of North Carolina at Chapel Hill, Chapel Hill, North Carolina 27599, United States; orcid.org/0000-0003-4122-7466

Jun Hu – Department of Chemistry, University of North Carolina at Chapel Hill, Chapel Hill, North Carolina 27599, United States; oorcid.org/0000-0002-6997-0174 Wei You — Department of Chemistry, University of North Carolina at Chapel Hill, Chapel Hill, North Carolina 27599, United States; Oorcid.org/0000-0003-0354-1948

Complete contact information is available at: https://pubs.acs.org/10.1021/acs.jpcc.1c00654

Author Contributions

[†]N.Z. and Z.O. made equal contributions.

Notes

The authors declare no competing financial interest.

Biographies

Ninghao Zhou is currently pursuing his Ph.D. under the supervision of Prof. Andrew M. Moran at the University of North Carolina Chapel Hill. He received his B.S. in chemistry from University of Science and Technology of China in 2016. His research interests focus on studying ultrafast dynamics in condensed-phase materials by nonlinear spectroscopic techniques.

Zhenyu Ouyang received his B.S. in Chemistry from the University of Science and Technology of China (Hefei, China) in 2018. He is currently a graduate student working in Prof. Moran's group in the Department of Chemistry at the University of North Carolina at Chapel Hill. His research focuses on the development of action spectroscopies for investigations of solar cell devices.

Meredith McNamee received a B.S. in Chemistry from North Carolina State University (Raleigh, NC) in 2019. McNamee is a graduate student in Prof. Moran's group in the Department of Chemistry at the University of North Carolina at Chapel Hill and focuses on developing spectroscopic methods to probe layered perovskite devices.

Olivia F. Williams earned her Ph.D. in physical chemistry from the University of North Carolina at Chapel Hill in Prof. Andrew Moran's research group. Her research involves the use of transient absorption microscopies to study carrier dynamics and exciton transport in semiconductor materials. Since earning her Ph.D. in May 2020, Olivia has joined Prof. Libai Huang's group at Purdue University as a postdoctoral research associate.

Zhenkun Guo received his B.S. in Chemistry from the University of Science and Technology of China (Hefei, China) in 2013 and received his Ph.D. in Chemistry from the University of North Carolina at Chapel Hill under the supervision of Prof. Moran. He is currently working as a scientist at Ultrafast Systems and is developing cutting-edge commercial time-resolved spectrometers.

Liang Yan obtained his B.S. degree in Polymer Science and Engineering at Tsinghua University, Beijing, in 2003, and his M.S. degree in Material Science at Tsinghua University, Beijing, in 2006. He received his Ph.D. degree from Prof. Bin Hu's group in Materials Science and Engineering at University of Tennessee at Knoxville in 2011. After that he started to work in Prof. Wei You's group as a Postdoctoral Research Associate and now as a Research Associate in the Department of Chemistry at University of North Carolina at Chapel Hill. His research focused on organic solar cell and low-dimensional organic—inorganic hybrid perovskites.

Jun Hu received his B.S. in Chemistry from Peking University in 2013. He received his Ph.D. in the Department of Chemistry at the University of North Carolina at Chapel Hill in 2018 and stayed as Postdoctoral Research Associate in 2019. During his time at the University of North Carolina at Chapel Hill, he worked in Professor Wei You's group and his research focused on the two-dimensional organic—inorganic hybrid perovskite solar cell. Currently Jun works in Applied Materials as a Process Engineer.

Wei You received his B.S. degree in Polymer Chemistry from University of Science and Technology of China (USTC) in 1999 and obtained his Ph.D. in 2004 under the guidance of Professor Luping Yu. He then moved west and finished his postdoctoral training at Stanford University in 2006 with Professor Zhenan Bao. In July 2006, Dr. You joined the University of North Carolina at Chapel Hill as an Assistant Professor in Chemistry and was promoted to the rank of Associate Professor in 2012 and then Full Professor in 2017. His research group focuses on (a) developing and fundamental understanding of novel materials for solar energy utilizations and (b) new polymeric materials based on novel polymerization methodologies for a variety of applications.

Andrew M. Moran earned a Ph.D. in Physical Chemistry from Kansas State University in 2002 under the direction of Professor Anne Myers Kelley. He then conducted research as a postdoctoral scholar with Professors Shaul Mukamel (University of Rochester), Kenneth Spears (Northwestern University), and Norbert Scherer (University of Chicago). Andrew arrived at the University of North Carolina in 2007 and is now an Associate Professor of Chemistry. Andrew's research group uses nonlinear optical and action spectroscopies to investigate carrier transport processes in photovoltaic materials.

ACKNOWLEDGMENTS

This work is supported by the National Science Foundation under CHE-1763207 (N.Z., Z.O., M.M., and A.M.M.). L.Y. and W.Y. acknowledge the support from UNC Research Opportunities Initiative (ROI) through the Center of Hybrid Materials Enabled Electronic Technology. Research of 2D perovskites fabrication was supported by the Center for Hybrid Organic Inorganic Semiconductors for Energy (CHOISE), an Energy Frontier Research Center funded by the U.S. Department of Energy (DOE), Office of Science, Office of Basic Energy Sciences (BES).

■ REFERENCES

- (1) Zhang, W.; Eperon, G. E.; Snaith, H. J. Metal Halide Perovskites for Energy Applications. *Nat. Energy* **2016**, *1* (6), 16048.
- (2) Yuan, M.; Quan, L. N.; Comin, R.; Walters, G.; Sabatini, R.; Voznyy, O.; Hoogland, S.; Zhao, Y.; Beauregard, E. M.; Kanjanaboos, P.; et al. Perovskite Energy Funnels for Efficient Light-Emitting Diodes. *Nat. Nanotechnol.* **2016**, *11* (10), 872–877.
- (3) Xing, J.; Zhao, Y.; Askerka, M.; Quan, L. N.; Gong, X.; Zhao, W.; Zhao, J.; Tan, H.; Long, G.; Gao, L.; et al. Color-Stable Highly Luminescent Sky-Blue Perovskite Light-Emitting Diodes. *Nat. Commun.* **2018**, *9* (1), 3541.
- (4) Smith, M. D.; Connor, B. A.; Karunadasa, H. I. Tuning the Luminescence of Layered Halide Perovskites. *Chem. Rev.* **2019**, *119* (5), 3104–3139.
- (5) Lin, Y.; Fang, Y.; Zhao, J.; Shao, Y.; Stuard, S. J.; Nahid, M. M.; Ade, H.; Wang, Q.; Shield, J. E.; Zhou, N.; et al. Unveiling the Operation Mechanism of Layered Perovskite Solar Cells. *Nat. Commun.* **2019**, *10* (1), 1008.
- (6) Lin, Y.-H.; Huang, W.; Pattanasattayavong, P.; Lin, J.; Li, R.; Sakai, N.; Panidi, J.; Hong, M. J.; Ma, C.; Wei, N.; et al. Deciphering Photocarrier Dynamics for Tuneable High-Performance Perovskite-Organic Semiconductor Heterojunction Phototransistors. *Nat. Commun.* **2019**, *10* (1), 4475.
- (7) Stoumpos, C. C.; Cao, D. H.; Clark, D. J.; Young, J.; Rondinelli, J. M.; Jang, J. I.; Hupp, J. T.; Kanatzidis, M. G. Ruddlesden—Popper Hybrid Lead Iodide Perovskite 2d Homologous Semiconductors. *Chem. Mater.* **2016**, 28 (8), 2852–2867.
- (8) Smith, M. D.; Crace, E. J.; Jaffe, A.; Karunadasa, H. I. The Diversity of Layered Halide Perovskites. *Annu. Rev. Mater. Res.* **2018**, 48 (1), 111–136.

- (9) Mauck, C. M.; Tisdale, W. A. Excitons in 2d Organic—Inorganic Halide Perovskites. *Trends Chem.* **2019**, *1*, 380–393.
- (10) Ren, H.; Yu, S.; Chao, L.; Xia, Y.; Sun, Y.; Zuo, S.; Li, F.; Niu, T.; Yang, Y.; Ju, H.; et al. Efficient and Stable Ruddlesden—Popper Perovskite Solar Cell with Tailored Interlayer Molecular Interaction. *Nat. Photonics* **2020**, *14* (3), 154–163.
- (11) Zheng, Y.; Niu, T.; Ran, X.; Qiu, J.; Li, B.; Xia, Y.; Chen, Y.; Huang, W. Unique Characteristics of 2d Ruddlesden—Popper (2drp) Perovskite for Future Photovoltaic Application. *J. Mater. Chem. A* **2019**, 7 (23), 13860—13872.
- (12) Smith, I. C.; Hoke, E. T.; Solis-Ibarra, D.; McGehee, M. D.; Karunadasa, H. I. A Layered Hybrid Perovskite Solar-Cell Absorber with Enhanced Moisture Stability. *Angew. Chem., Int. Ed.* **2014**, *53* (42), 11232–11235.
- (13) Niu, G.; Guo, X.; Wang, L. Review of Recent Progress in Chemical Stability of Perovskite Solar Cells. *J. Mater. Chem. A* **2015**, 3 (17), 8970–8980.
- (14) Liu, J.; Leng, J.; Wu, K.; Zhang, J.; Jin, S. Observation of Internal Photoinduced Electron and Hole Separation in Hybrid Two-Dimentional Perovskite Films. *J. Am. Chem. Soc.* **2017**, *139* (4), 1432–1435.
- (15) Shang, Q.; Wang, Y.; Zhong, Y.; Mi, Y.; Qin, L.; Zhao, Y.; Qiu, X.; Liu, X.; Zhang, Q. Unveiling Structurally Engineered Carrier Dynamics in Hybrid Quasi-Two-Dimensional Perovskite Thin Films toward Controllable Emission. *J. Phys. Chem. Lett.* **2017**, 8 (18), 4431–4438.
- (16) Blancon, J. C.; Tsai, H.; Nie, W.; Stoumpos, C. C.; Pedesseau, L.; Katan, C.; Kepenekian, M.; Soe, C. M. M.; Appavoo, K.; Sfeir, M. Y.; et al. Extremely Efficient Internal Exciton Dissociation through Edge States in Layered 2d Perovskites. *Science* **2017**, 355 (6331), 1288
- (17) Williams, O. F.; Guo, Z.; Hu, J.; Yan, L.; You, W.; Moran, A. M. Energy Transfer Mechanisms in Layered 2d Perovskites. *J. Chem. Phys.* **2018**, *148* (13), 134706.
- (18) Yan, L.; Hu, J.; Guo, Z.; Chen, H.; Toney, M. F.; Moran, A. M.; You, W. General Post-Annealing Method Enables High-Efficiency Two-Dimensional Perovskite Solar Cells. *ACS Appl. Mater. Interfaces* **2018**, *10* (39), 33187–33197.
- (19) Proppe, A. H.; Elkins, M. H.; Voznyy, O.; Pensack, R. D.; Zapata, F.; Besteiro, L. V.; Quan, L. N.; Quintero-Bermudez, R.; Todorovic, P.; Kelley, S. O.; et al. Spectrally Resolved Ultrafast Exciton Transfer in Mixed Perovskite Quantum Wells. *J. Phys. Chem. Lett.* **2019**, *10* (3), 419–426.
- (20) Lin, D.; Ma, L.; Ni, W.; Wang, C.; Zhang, F.; Dong, H.; Gurzadyan, G. G.; Nie, Z. Unveiling Hot Carrier Relaxation and Carrier Transport Mechanisms in Quasi-Two-Dimensional Layered Perovskites. J. Mater. Chem. A 2020, 8 (47), 25402–25410.
- (21) Gan, Z.; Chen, W.; Zhou, C.; Yu, L.; Dong, L.; Jia, B.; Wen, X. Efficient Energy Funnelling by Engineering the Bandgap of a Perovskite: Förster Resonance Energy Transfer or Charge Transfer? *J. Phys. Chem. Lett.* **2020**, *11* (15), 5963–5971.
- (22) Fakharuddin, A.; Franckevičius, M.; Devižis, A.; Gelžinis, A.; Chmeliov, J.; Heremans, P.; Gulbinas, V. Double Charge Transfer Dominates in Carrier Localization in Low Bandgap Sites of Heterogeneous Lead Halide Perovskites. *Adv. Funct. Mater.* **2021**, 2010076
- (23) Zhou, N.; Hu, J.; Ouyang, Z.; Williams, O. F.; Yan, L.; You, W.; Moran, A. M. Nonlinear Photocurrent Spectroscopy of Layered 2d Perovskite Quantum Wells. *J. Phys. Chem. Lett.* **2019**, *10* (23), 7362–7367.
- (24) Zhou, N.; Ouyang, Z.; Hu, J.; Williams, O. F.; Yan, L.; You, W.; Moran, A. M. Distinguishing Energy- and Charge-Transfer Processes in Layered Perovskite Quantum Wells with Two-Dimensional Action Spectroscopies. *J. Phys. Chem. Lett.* **2020**, *11* (12), 4570–4577.
- (25) Ouyang, Z.; Zhou, N.; Hu, J.; Williams, O. F.; Yan, L.; You, W.; Moran, A. M. Nonlinear Fluorescence Spectroscopy of Layered Perovskite Quantum Wells. *J. Chem. Phys.* **2020**, *153* (13), 134202.
- (26) Zhou, N.; Ouyang, Z.; Yan, L.; McNamee, M. G.; You, W.; Moran, A. M. Elucidation of Quantum-Well-Specific Carrier

- Mobilities in Layered Perovskites. J. Phys. Chem. Lett. 2021, 12, 1116-1123.
- (27) Lanzani, G; Zenz, C; Cerullo, G; Graupner, W; Leising, G; Scherf, U; De Silvestri, S Femtosecond Photovoltage Excitation Cross-Correlation on a Ladder-Type Polymer. *Synth. Met.* **2000**, 111–112, 493–496.
- (28) Bakulin, A. A.; Rao, A.; Pavelyev, V. G.; van Loosdrecht, P. H. M.; Pshenichnikov, M. S.; Niedzialek, D.; Cornil, J.; Beljonne, D.; Friend, R. H. The Role of Driving Energy and Delocalized States for Charge Separation in Organic Semiconductors. *Science* **2012**, 335 (6074), 1340.
- (29) Nardin, G.; Autry, T. M.; Silverman, K. L.; Cundiff, S. T. Multidimensional Coherent Photocurrent Spectroscopy of a Semi-conductor Nanostructure. *Opt. Express* **2013**, *21* (23), 28617–28627.
- (30) Karki, K. J.; Widom, J. R.; Seibt, J.; Moody, I.; Lonergan, M. C.; Pullerits, T.; Marcus, A. H. Coherent Two-Dimensional Photocurrent Spectroscopy in a Pbs Quantum Dot Photocell. *Nat. Commun.* **2014**, 5 (1), 5869.
- (31) Bakulin, A. A.; Silva, C.; Vella, E. Ultrafast Spectroscopy with Photocurrent Detection: Watching Excitonic Optoelectronic Systems at Work. *J. Phys. Chem. Lett.* **2016**, 7 (2), 250–258.
- (32) Tiwari, V.; Matutes, Y. A.; Konar, A.; Yu, Z.; Ptaszek, M.; Bocian, D. F.; Holten, D.; Kirmaier, C.; Ogilvie, J. P. Strongly Coupled Bacteriochlorin Dyad Studied Using Phase-Modulated Fluorescence-Detected Two-Dimensional Electronic Spectroscopy. *Opt. Express* **2018**, *26* (17), 22327–22341.
- (33) Malý, P.; Mančal, T. Signatures of Exciton Delocalization and Exciton–Exciton Annihilation in Fluorescence-Detected Two-Dimensional Coherent Spectroscopy. *J. Phys. Chem. Lett.* **2018**, 9 (19), 5654–5659.
- (34) Mueller, S.; Draeger, S.; Ma, X.; Hensen, M.; Kenneweg, T.; Pfeiffer, W.; Brixner, T. Fluorescence-Detected Two-Quantum and One-Quantum—Two-Quantum 2d Electronic Spectroscopy. *J. Phys. Chem. Lett.* **2018**, *9* (8), 1964–1969.
- (35) Guo, Z.; Zhou, N.; Williams, O. F.; Hu, J.; You, W.; Moran, A. M. Imaging Carrier Diffusion in Perovskites with a Diffractive Optic-Based Transient Absorption Microscope. *J. Phys. Chem. C* **2018**, *122* (19), 10650–10656.
- (36) Williams, O. F.; Zhou, N.; Hu, J.; Ouyang, Z.; Kumbhar, A.; You, W.; Moran, A. M. Imaging Excited State Dynamics in Layered 2d Perovskites with Transient Absorption Microscopy. *J. Phys. Chem. A* **2019**, *123* (51), 11012–11021.
- (37) Zaslow, B.; Zandler, M. E. Two-Dimensional Analog to the Hydrogen Atom. *Am. J. Phys.* **1967**, *35* (12), 1118–1119.
- (38) Blancon, J. C.; Stier, A. V.; Tsai, H.; Nie, W.; Stoumpos, C. C.; Traoré, B.; Pedesseau, L.; Kepenekian, M.; Katsutani, F.; Noe, G. T.; et al. Scaling Law for Excitons in 2d Perovskite Quantum Wells. *Nat. Commun.* **2018**, *9* (1), 2254.
- (39) Zhang, L.; Zhang, X.; Lu, G. Band Alignment in Two-Dimensional Halide Perovskite Heterostructures: Type I or Type Ii? *J. Phys. Chem. Lett.* **2020**, *11* (8), 2910–2916.
- (40) Kubo, R. The Fluctuation-Dissipation Theorem. *Rep. Prog. Phys.* **1966**, 29 (1), 255–284.
- (41) Guo, Z.; Manser, J. S.; Wan, Y.; Kamat, P. V.; Huang, L. Spatial and Temporal Imaging of Long-Range Charge Transport in Perovskite Thin Films by Ultrafast Microscopy. *Nat. Commun.* **2015**, *6* (1), 7471.
- (42) Tian, W.; Zhao, C.; Leng, J.; Cui, R.; Jin, S. Visualizing Carrier Diffusion in Individual Single-Crystal Organolead Halide Perovskite Nanowires and Nanoplates. *J. Am. Chem. Soc.* **2015**, *137* (39), 12458–12461.
- (43) Beane, G.; Devkota, T.; Brown, B. S.; Hartland, G. V. Ultrafast Measurements of the Dynamics of Single Nanostructures: A Review. *Rep. Prog. Phys.* **2019**, 82 (1), 016401.
- (44) Hill, A. H.; Kennedy, C. L.; Massaro, E. S.; Grumstrup, E. M. Perovskite Carrier Transport: Disentangling the Impacts of Effective Mass and Scattering Time through Microscopic Optical Detection. *J. Phys. Chem. Lett.* **2018**, 9 (11), 2808–2813.

- (45) Van Goethem, E. M.; Pinion, C. W.; Cating, E. E. M.; Cahoon, J. F.; Papanikolas, J. M. Observation of Phonon Propagation in Germanium Nanowires Using Femtosecond Pump—Probe Microscopy. ACS Photonics 2019, 6 (9), 2213—2222.
- (46) Jones, A. C.; Kearns, N. M.; Bohlmann Kunz, M.; Flach, J. T.; Zanni, M. T. Multidimensional Spectroscopy on the Microscale: Development of a Multimodal Imaging System Incorporating 2d White-Light Spectroscopy, Broadband Transient Absorption, and Atomic Force Microscopy. *J. Phys. Chem. A* **2019**, *123* (50), 10824–10836.
- (47) Steves, M. A.; Zheng, H.; Knappenberger, K. L. Correlated Spatially Resolved Two-Dimensional Electronic and Linear Absorption Spectroscopy. *Opt. Lett.* **2019**, *44* (8), 2117–2120.
- (48) Ginsberg, N. S.; Tisdale, W. A. Spatially Resolved Photogenerated Exciton and Charge Transport in Emerging Semiconductors. *Annu. Rev. Phys. Chem.* **2020**, 71 (1), 1–30.
- (49) Hickey, C. L.; Grumstrup, E. M. Reduced Artifact Approach for Determining Diffusion Coefficients in Time-Resolved Microscopy. *J. Phys. Chem. C* **2020**, *124* (25), 14016–14021.
- (50) Jiang, X.; Jun, S.; Hoffman, J.; Kanatzidis, M. G.; Harel, E. Global Analysis for Time and Spectrally Resolved Multidimensional Microscopy: Application to Ch3nh3pbi3 Perovskite Thin Films. *J. Phys. Chem. A* **2020**, *124* (23), 4837–4847.
- (51) Huang, L.; Wong, C.; Grumstrup, E. Time-Resolved Microscopy: A New Frontier in Physical Chemistry. *J. Phys. Chem.* A 2020, 124 (29), 5997–5998.
- (52) Blake, M. J.; Colon, B. A.; Calhoun, T. R. Leaving the Limits of Linearity for Light Microscopy. J. Phys. Chem. C 2020, 124 (45), 24555–24565.
- (53) Hill, A. H.; Smyser, K. E.; Kennedy, C. L.; Massaro, E. S.; Grumstrup, E. M. Screened Charge Carrier Transport in Methylammonium Lead Iodide Perovskite Thin Films. *J. Phys. Chem. Lett.* **2017**, *8* (5), 948–953.
- (54) Landsberg, P. T. Recombination in Semiconductors; Cambridge University Press: Cambridge, 1991.
- (55) Mukamel, S.; Abramavicius, D. Many-Body Approaches for Simulating Coherent Nonlinear Spectroscopies of Electronic and Vibrational Excitons. *Chem. Rev.* **2004**, *104* (4), 2073–2098.
- (56) Schlau-Cohen, G. S.; Ishizaki, A.; Fleming, G. R. Two-Dimensional Electronic Spectroscopy and Photosynthesis: Fundamentals and Applications to Photosynthetic Light-Harvesting. *Chem. Phys.* **2011**, 386 (1), 1–22.
- (57) Hong, X.; Ishihara, T.; Nurmikko, A. V. Dielectric Confinement Effect on Excitons in Pb₄-Based Layered Semiconductors. *Phys. Rev. B: Condens. Matter Mater. Phys.* **1992**, 45 (12), 6961–6964.
- (58) Barbara, P. F.; Meyer, T. J.; Ratner, M. A. Contemporary Issues in Electron Transfer Research. *J. Phys. Chem.* **1996**, *100* (31), 13148–13168.
- (59) Nitzan, A. Chemical Dynamics in Condensed Phases; Oxford University Press: Oxford, 2006.
- (60) Jia, Y.; Jean, J. M.; Werst, M. M.; Chan, C. K.; Fleming, G. R. Simulations of the Temperature Dependence of Energy Transfer in the Psi Core Antenna. *Biophys. J.* **1992**, *63* (1), 259–273.
- (61) Savikhin, S.; van Amerongen, H.; Kwa, S. L.; van Grondelle, R.; Struve, W. S. Low-Temperature Energy Transfer in Lhc-Ii Trimers from the Chl a/B Light-Harvesting Antenna of Photosystem Ii. *Biophys. J.* **1994**, *66* (5), 1597–1603.
- (62) Gaab, K. M.; Bardeen, C. J. Wavelength and Temperature Dependence of the Femtosecond Pump—Probe Anisotropies in the Conjugated Polymer Meh-Ppv: Implications for Energy-Transfer Dynamics. J. Phys. Chem. B 2004, 108 (15), 4619—4626.
- (63) Mukamel, S. Principles of Nonlinear Optical Spectroscopy; Oxford University Press: New York, 1995.
- (64) Tokmakoff, A. Time-Dependent Quantum Mechanics and Spectroscopy; University of Chicago, 2021; http://tdqms.uchicago.edu/.
- (65) Spear, W. E. Drift Mobility Techniques for the Study of Electrical Transport Properties in Insulating Solids. *J. Non-Cryst. Solids* **1969**, *1* (3), 197–214.

- (66) Dong, Q.; Fang, Y.; Shao, Y.; Mulligan, P.; Qiu, J.; Cao, L.; Huang, J. Electron-Hole Diffusion Lengths > 175 Mm in Solution-Grown Ch3nh3pbi3 Single Crystals. *Science* **2015**, 347 (6225), 967.
- (67) Shi, D.; Adinolfi, V.; Comin, R.; Yuan, M.; Alarousu, E.; Buin, A.; Chen, Y.; Hoogland, S.; Rothenberger, A.; Katsiev, K.; et al. Low Trap-State Density and Long Carrier Diffusion in Organolead Trihalide Perovskite Single Crystals. *Science* **2015**, 347, 519–522.
- (68) Alvar, M. S.; Blom, P. W. M.; Wetzelaer, G.-J. A. H. Space-Charge-Limited Electron and Hole Currents in Hybrid Organic-Inorganic Perovskites. *Nat. Commun.* **2020**, *11*, 4023.
- (69) Xing, G.; Mathews, N.; Sun, S.; Lim, S. S.; Lam, Y. M.; Grätzel, M.; Mhaisalkar, S. G.; Sum, T. C. Long-Range Balanced Electron- and Hole-Transport Lengths in Organic-Inorganic Ch₃nh₃pbi₃. *Science* **2013**, 342, 344–347.
- (70) Mitzi, D. B.; Chondroudis, K.; Kagan, C. R. Design, Structure, and Optical Properties of Organic–Inorganic Perovskites Containing an Oligothiophene Chromophore. *Inorg. Chem.* **1999**, 38 (26), 6246–6256.
- (71) Chondroudis, K.; Mitzi, D. B. Electroluminescence from an Organic–Inorganic Perovskite Incorporating a Quaterthiophene Dye within Lead Halide Perovskite Layers. *Chem. Mater.* **1999**, *11* (11), 3028–3030
- (72) Jemli, K.; Audebert, P.; Galmiche, L.; Trippé-Allard, G.; Garrot, D.; Lauret, J.-S.; Deleporte, E. Two-Dimensional Perovskite Activation with an Organic Luminophore. *ACS Appl. Mater. Interfaces* **2015**, 7 (39), 21763–21769.
- (73) Passarelli, J. V.; Fairfield, D. J.; Sather, N. A.; Hendricks, M. P.; Sai, H.; Stern, C. L.; Stupp, S. I. Enhanced out-of-Plane Conductivity and Photovoltaic Performance in N = 1 Layered Perovskites through Organic Cation Design. *J. Am. Chem. Soc.* **2018**, *140* (23), 7313–7323.
- (74) Liu, C.; Huhn, W.; Du, K.-Z.; Vazquez-Mayagoitia, A.; Dirkes, D.; You, W.; Kanai, Y.; Mitzi, D. B.; Blum, V. Tunable Semi-conductors: Control over Carrier States and Excitations in Layered Hybrid Organic-Inorganic Perovskites. *Phys. Rev. Lett.* **2018**, *121* (14), 146401.
- (75) Hu, J.; Oswald, I. W. H.; Hu, H.; Stuard, S. J.; Nahid, M. M.; Yan, L.; Chen, Z.; Ade, H.; Neilson, J. R.; You, W. Aryl-Perfluoroaryl Interaction in Two-Dimensional Organic—Inorganic Hybrid Perovskites Boosts Stability and Photovoltaic Efficiency. *ACS Mater. Lett.* **2019**, *1* (1), 171–176.